

# An Analysis of the DS-CDMA Cellular Uplink for Arbitrary and Constrained Topologies

Don Torrieri, *Senior Member, IEEE*, Matthew C. Valenti, *Senior Member, IEEE*,  
and Salvatore Talarico, *Student Member, IEEE*.

**Abstract**—A new analysis is presented for the direct-sequence code-division multiple access (DS-CDMA) cellular uplink. For a given network topology, closed-form expressions are found for the outage probability and rate of each uplink in the presence of path-dependent Nakagami fading and shadowing. The topology may be arbitrary or modeled by a random spatial distribution with a fixed number of base stations and mobiles placed over a finite area. The analysis is more detailed and accurate than existing ones and facilitates the resolution of network design issues including the influence of the minimum base-station separation, the role of the spreading factor, and the impact of various power-control and rate-control policies. It is shown that once power control is established, the rate can be allocated according to a fixed-rate or variable-rate policy with the objective of either meeting an outage constraint or maximizing throughput. An advantage of variable-rate power control is that it allows an outage constraint to be enforced on every uplink, which is impossible when a fixed rate is used throughout the network.

**Index Terms**—CDMA, cellular network, uplink, power control, rate control

## I. INTRODUCTION

THE classical analysis of the cellular uplinks (e.g., [1]–[3]) in a cellular network entails a number of questionable assumptions, including the existence of a lattice or regular grid of base stations and the modeling of intercell interference at a base station as a fixed fraction of the total interference. Although conceptually simple and locally tractable, the grid assumption is a poor model for actual base-station deployments, which cannot assume a regular grid structure due to a variety of regulatory and physical constraints. The intercell-interference assumption is untenable because the fractional proportion of intercell interference varies substantially with the mobile and base-station locations, the shadowing, and the fading.

More recent analyses of cellular networks (e.g., [4]–[6]) locate the mobiles and/or the base stations according to a two-dimensional Poisson point process (PPP) over a network that extends infinitely on the Euclidian plane, thereby allowing

the use of analytical tools from stochastic geometry [7]–[9]. Although the two principal limitations of the classical approach are eliminated, the PPP approach is still unrealistic because it does not permit a minimum separation between base stations or between mobiles, although both minimum separations are characteristic of actual macro-cellular deployments. Other problems with the PPP model are that no network has an infinite area and that any realization of a PPP could have an implausibly large number of mobiles or base stations placed within a finite area.

The cellular downlink is considered in [4] and [5], while the cellular uplink is considered in [6]. The model for the uplink proposed in [6] involves drawing the locations of the mobiles from a PPP and then locating the base station for each mobile uniformly in the mobile’s Voronoi cell. This model supposes a one-to-one relationship between mobiles and base stations and therefore cannot be used to model networks that allow several simultaneous connections per base station. In [5], it is shown that when the variance of the lognormal shadowing is large, the PPP model is a reasonable approximation even for a network with base stations located on a regular lattice. However, in these works the shadowing and fading are lumped into a single variable, which confounds their relative contributions. In particular, shadowing affects the base-station selection, but fading does not. A key motivation of the present paper is to separately account for the shadowing and fading.

The goal of this paper is to provide a new and accurate analysis of the direct-sequence code-division multiple-access (DS-CDMA) uplink. The analysis can be used to determine the exact outage probability of an arbitrary fixed topology with no need for simulation. In addition, a constrained spatial model is introduced, which imposes a minimum separation among base stations. The minimum separation can be selected to match the observed locations of an actual cellular deployment. Analytical techniques are presented for characterizing the performance of networks drawn from the constrained spatial model. The model facilitates the observation of certain phenomena. For instance, it is shown subsequently in Fig. 9 that the minimum separation between base stations has a significant effect on area spectral efficiency. Another benefit of the analysis is that it exposes the tradeoffs entailed in choosing among various power-control and rate-control policies in terms of both the outage probabilities and the area spectral efficiencies.

The analysis in this paper applies a closed-form expression [10] for the *conditional* outage probability of a communication link, where the conditioning is with respect to an arbitrary realization of the network topology. The techniques of [10]

Portions of this work were presented at the IEEE International Conference on Communications (ICC), Budapest, Hungary, June 2013.

M. C. Valenti’s work was sponsored by the National Science Foundation under Award No. CNS-0750821 and by the United States Army Research Laboratory under Contract W911NF-10-0109.

D. Torrieri is with the US Army Research Laboratory, Adelphi, MD (email: don.j.torrieri.civ@mail.mil).

M. C. Valenti and S. Talarico are with West Virginia University, Morgantown, WV, U.S.A. (email: valenti@ieee.org, Salvatore.Talarico81@gmail.com).

Digital Object Identifier 10.1109/TCOMM.2013.13.120911

are adapted to provide the uplink outage probability of an arbitrary DS-CDMA uplink in closed form with no need to simulate the corresponding channels. A Nakagami- $m$  fading model is assumed, which models a wide class of channels, and the fading parameters do not need to be identical for all communication links. This flexibility allows the modeling of distance-dependent fading, where mobiles close to the base station have a dominant line-of-sight path, but the more distant mobiles do not.

Although our analysis is applicable for arbitrary topologies, we focus on modeling the network with a constrained spatial model. The spatial model places a fixed number of base stations within a region of finite extent. The model enforces a minimum separation among the base stations for each *network realization*, which comprises a base-station placement, a mobile placement, and a shadowing realization. The model for both mobile and base-station placement is the *uniform-clustering* model [10], which entails a uniformly distributed placement within the network after certain regions around mobiles and base stations have been excluded. To characterize the performance of the constrained spatial model, realizations of the network are drawn according to the desired spatial and shadowing models, and the computed outage probabilities are collected. These outage probabilities can be used to characterize the average uplink performance. Alternatively, the outage probability of each uplink can be constrained, and the statistics of the rate provided to each mobile for its uplink can be determined under various resource-allocation policies.

A DS-CDMA uplink differs from a downlink, which has been presented in a separate paper [11], in at least four significant ways. First, the sources of interference are many mobiles for the uplink whereas the sources are a few base stations for the downlink. Second, the uplink signals arriving at a base station are asynchronous. Therefore, they are not orthogonal and intracell interference can not be ignored. Third, sectorization is a critical factor in uplink performance whereas it is of minor importance in downlink performance. Fourth, because base stations are equipped with better transmit high-power amplifiers and receive low-noise amplifiers than the mobiles, the operational signal-to-noise ratio is typically 5-10 dB lower for the uplink than for the downlink.

The remainder of this paper is organized as follows. Section II presents a model of the network culminating in an expression for SINR in Section III. Section IV adapts the expression for outage probability published in [10] to the analysis of an arbitrary DS-CDMA uplink. Section V discusses policies for power control, rate control, and cell association/reselection. A performance analysis given in Section VI compares several network policies on the basis of outage probability, throughput, area spectral efficiency, and fairness. The section also investigates the influence of the spreading factor, minimum base-station separation, and base-station reselection policy.

## II. NETWORK MODEL

A *sector* is defined as the range of angles from which a directional sector antenna can receive signals. A mobile within the sector of a sector antenna is said to be *covered* by the sector

antenna. Cells may be divided into sectors by using several directional sector antennas or arrays, each covering disjoint angles, at the base stations. Only mobiles in the directions covered by a sector antenna can cause intracell or intercell multiple-access interference on the *uplink* from a mobile to its associated sector antenna. Thus, the number of interfering signals on an uplink is reduced approximately by a factor equal to the number of sectors. Practical sector antennas have patterns with sidelobes that extend into adjacent sectors, but the performance degradation due to overlapping sectors is significant only for a small percentage of mobile locations. Three ideal sector antennas and sectors per base station, each covering  $2\pi/3$  radians, are assumed in the subsequent analysis. The mobile antennas are assumed to be omnidirectional.

The network comprises  $C$  base stations and cells,  $3C$  sectors  $\{S_1, \dots, S_{3C}\}$ , and  $M$  mobiles  $\{X_1, \dots, X_M\}$ . The base stations and mobiles are confined to a finite area, which is assumed to be a circle of radius  $r_{\text{net}}$  and area  $\pi r_{\text{net}}^2$ . The sector boundary angles are the same for all base stations. The variable  $S_j$  represents both the  $j^{\text{th}}$  sector antenna and its location, and  $X_i$  represents the  $i^{\text{th}}$  mobile and its location.

An *exclusion zone* of radius  $r_{\text{bs}}$  surrounds each base station, and no other base stations are allowed within this zone. Similarly, an exclusion zone of radius  $r_{\text{m}}$  surrounds each mobile where no other mobiles are allowed. The minimum separation between mobiles is generally much smaller than the minimum separation between the base stations. Base-station exclusion zones are primarily determined by economic considerations and the terrain, whereas mobile exclusion zones are determined by the need to avoid physical collision. The value of  $r_{\text{bs}}$  could be empirically determined by examining the locations of base stations in a real network. The value of  $r_{\text{bs}}$  could be selected to provide the best statistical fit. This procedure is similar to determining values for fading and shadowing parameters by statistically fitting actual data.

Example network topologies are shown in Fig. 1. The top subfigure shows the locations of actual base stations in a small city with hilly terrain. The base-station locations are given by the large filled circles, and the Voronoi cells are indicated in the figure. The minimum base-station separation is observed to be about 0.43 km. The bottom subfigure shows a portion of a randomly generated network with average number of mobiles per cell  $M/C = 16$ , a base-station exclusion radius  $r_{\text{bs}} = 0.25$ , and a mobile exclusion radius  $r_{\text{m}} = 0.01$ . The locations of the mobiles are represented by small dots, and lines indicate the angular coverage of sector antennas. The topological similarity of the two subfigures supports the use of the uniform-clustering model.

## III. SINR

Consider a reference receiver of a sector antenna that receives a desired signal from a reference mobile within its cell and sector. Both intracell and intercell interference are received from other mobiles within the covered angle of the sector, but interference from mobiles in extraneous sectors is negligible. The varying propagation delays from the interfering mobiles cause their interference signals to be asynchronous with respect to the desired signal.

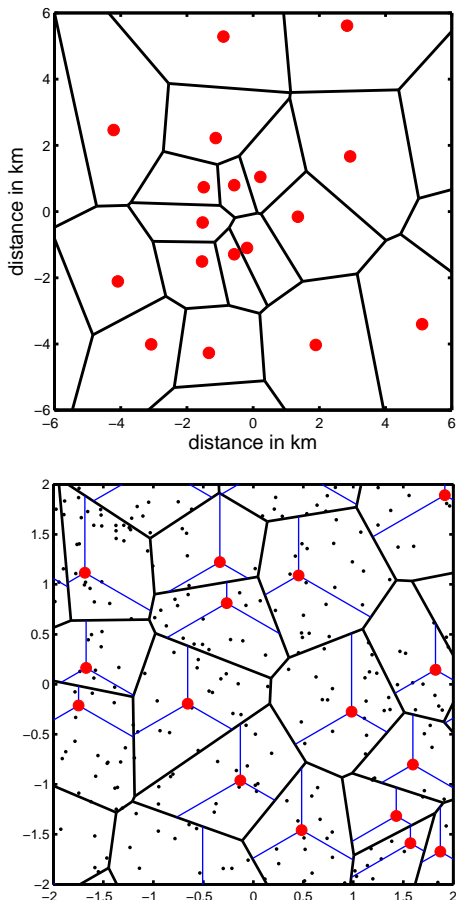


Fig. 1. Example network topologies. Base stations are represented by large circles, and cell boundaries are represented by thick lines. Top subfigure: Actual base station locations from a current cellular deployment. Bottom subfigure: Simulated base-station locations using a base-station exclusion zone  $r_{bs} = 0.25$ . In the bottom subfigure, the simulated positions of the mobiles are represented by small dots, the sector boundaries are represented by light lines, and the average cell load is  $M/C = 16$  mobiles.

In a DS-CDMA network of asynchronous quadriphase direct-sequence systems, a multiple-access interference signal with power  $I$  before despreading is reduced after despreading to the power level  $Ih(\tau_o)/G$ , where  $G$  is the processing gain or spreading factor, and  $h(\tau_o)$  is a function of the chip waveform and the timing offset  $\tau_o$  of the interference spreading sequence relative to that of the desired or reference signal. If  $\tau_o$  is assumed to have a uniform distribution over  $[0, T_c]$ , then the expected value of  $h(\tau_o)$  is the chip factor  $h$ . For rectangular chip waveforms,  $h = 2/3$  [12], [13]. It is assumed henceforth that  $G/h(\tau_o)$  is a constant equal to  $G/h$  at each sector receiver.

Let  $\mathcal{A}_j$  denote the set of mobiles covered by sector antenna  $S_j$ . A mobile  $X_i \in \mathcal{A}_j$  will be associated with  $S_j$  if the mobile's signal is received at  $S_j$  with a higher average power than at any other sector antenna in the network. Let  $\mathcal{X}_j \subset \mathcal{A}_j$  denote the set of mobiles associated with sector antenna  $S_j$ . Let  $X_r \in \mathcal{X}_j$  denote a reference mobile that transmits a desired signal to  $S_j$ . The power of  $X_r$  received at  $S_j$  is not significantly affected by the spreading factor and depends on the fading and path-loss models. The power of  $X_i$ ,  $i \neq r$ , received at  $S_j$  is nonzero only if  $X_i \in \mathcal{A}_j$ , is reduced by  $G/h$ , and also depends on the fading and path-loss models. We assume that path loss has a power-law dependence on

distance and is perturbed by shadowing. When accounting for fading and path loss, the despread instantaneous power of  $X_i$  received at  $S_j$  is

$$\rho_{i,j} = \begin{cases} P_r g_{r,j} 10^{\xi_{r,j}/10} f(\|S_j - X_r\|) & i = r \\ \left(\frac{h}{G}\right) P_i g_{i,j} 10^{\xi_{i,j}/10} f(\|S_j - X_i\|) & i : X_i \in \mathcal{A}_j \setminus X_r \\ 0 & i : X_i \notin \mathcal{A}_j \end{cases} \quad (1)$$

where  $g_{i,j}$  is the power gain due to fading,  $\xi_{i,j}$  is a shadowing factor,  $P_i$  is the power transmitted by  $X_i$ , and  $\mathcal{A}_j \setminus X_r$  is set  $\mathcal{A}_j$  with element  $X_r$  removed. The  $\{g_{i,j}\}$  are independent with unit-mean, and  $g_{i,j} = a_{i,j}^2$ , where  $a_{i,j}$  has a Nakagami distribution with parameter  $m_{i,j}$ . While the  $\{g_{i,j}\}$  are independent from each mobile to each base station, they are not necessarily identically distributed, and each link can have a distinct  $m_{i,j}$ . When the channel between  $S_j$  and  $X_i$  experiences Rayleigh fading,  $m_{i,j} = 1$  and  $g_{i,j}$  is exponentially distributed. In the presence of lognormal shadowing, the  $\{\xi_{i,j}\}$  are i.i.d. zero-mean Gaussian random variables with variance  $\sigma_s^2$ . In the absence of shadowing,  $\xi_{i,j} = 0$ . The path-loss function is expressed as the attenuation power law

$$f(d) = \left(\frac{d}{d_0}\right)^{-\alpha}, \quad d \geq d_0, \quad (2)$$

where  $\alpha \geq 2$  is the attenuation power-law exponent, and  $d_0$  is sufficiently large that the signals are in the far field. It is assumed that no mobiles are within distance  $d_0$  of any base station.

It is assumed that the  $\{g_{i,j}\}$  remain fixed for the duration of a time interval, but vary independently from interval to interval (block fading). With probability  $p_i$ , the  $i^{\text{th}}$  interferer transmits in the same time interval as the reference signal. The activity probability  $p_i$  can be used to model voice-activity factors or controlled silence. Although the  $\{p_i\}$  need not be the same, it is assumed that they are identical in the subsequent examples.

Let  $g(i)$  denote a function that returns the index of the sector antenna serving  $X_i$  so that  $X_i \in \mathcal{X}_j$  if  $g(i) = j$ . Usually, the sector antenna  $S_{g(i)}$  that serves mobile  $X_i$  is selected to be the one with index

$$g(i) = \underset{j}{\operatorname{argmax}} \left\{ 10^{\xi_{i,j}/10} f(\|S_j - X_i\|), X_i \in \mathcal{A}_j \right\} \quad (3)$$

which is the sector antenna with minimum path loss from  $X_i$  among those that cover  $X_i$ . In the absence of shadowing, it will be the sector antenna that is closest to  $X_i$ . In the presence of shadowing, a mobile may actually be associated with a sector antenna that is more distant than the closest one if the shadowing conditions are sufficiently better.

The instantaneous SINR at sector antenna  $S_j$  when the desired signal is from  $X_r \in \mathcal{X}_j$  is

$$\gamma_{r,j} = \frac{\rho_{r,j}}{\mathcal{N} + \sum_{i=1, i \neq r}^M I_i \rho_{i,j}} \quad (4)$$

where  $\mathcal{N}$  is the noise power,  $M$  is the number of mobiles, and  $I_i$  is a Bernoulli variable with probability  $P[I_i = 1] = p_i$

and  $P[I_i = 0] = 1 - p_i$ . Substituting (1) and (2) into (4) yields

$$\gamma_{r,j} = \frac{g_{r,j}\Omega_{r,j}}{\Gamma^{-1} + \sum_{i=1, i \neq r}^M I_i g_{i,j} \Omega_{i,j}} \quad (5)$$

where  $\Gamma = d_0^\alpha P_r / \mathcal{N}$  is the signal-to-noise ratio (SNR) due to a mobile located at unit distance when fading and shadowing are absent, and

$$\Omega_{i,j} = \begin{cases} 10^{\xi_{r,j}/10} \|S_j - X_r\|^{-\alpha} & i = r \\ \frac{h P_i}{G P_r} 10^{\xi_{i,j}/10} \|S_j - X_i\|^{-\alpha} & i : X_i \in \mathcal{A}_j \setminus X_r \\ 0 & i : X_i \notin \mathcal{A}_j \end{cases} \quad (6)$$

is the normalized mean despread power of  $X_i$  received at  $S_j$ , where the normalization is by  $P_r$ . The set of  $\{\Omega_{i,j}\}$  for reference receiver  $S_j$  is represented by  $\Omega_j = \{\Omega_{1,j}, \dots, \Omega_{M,j}\}$ .

#### IV. OUTAGE PROBABILITY

Let  $\beta_r$  denote the minimum instantaneous SINR required for reliable reception of a signal from  $X_r$  at its serving sector antenna. An *outage* occurs when the SINR of a signal from  $X_r$  falls below  $\beta_r$ . The value of  $\beta_r$  is a function of the *rate*  $R_r$  of the uplink. The relationship  $R_r = C(\beta_r)$  depends on the modulation and coding schemes used, and typically only a discrete set of  $R_r$  can be selected. While the exact dependence of  $R_r$  on  $\beta_r$  can be determined empirically through tests or simulation, we make the simplifying assumption when computing our numerical results that  $C(\beta_r) = \log_2(1 + \beta_r)$  corresponding to the Shannon capacity for complex discrete-time AWGN channels. This assumption is fairly accurate for modern cellular systems, which use turbo codes with a large number of available rates.

Conditioning on  $\Omega_j$ , the outage probability of a desired signal from  $X_r \in \mathcal{X}_j$  that arrives at  $S_j, j = \mathbf{g}(r)$ , is

$$\epsilon_r = P[\gamma_{r,j} \leq \beta_r | \Omega_j]. \quad (7)$$

Because it is conditioned on  $\Omega_j$ , the outage probability depends on the particular network realization, which has dynamics over timescales that are much slower than the fading. In [10], it is proved that

$$\epsilon_r = 1 - e^{-\beta_0 z} \sum_{s=0}^{m_0-1} (\beta_0 z)^s \sum_{t=0}^s \frac{z^{-t} H_t(\Psi)}{(s-t)!} \quad (8)$$

where  $m_0 = m_{r,j}$  is an integer,  $\beta_0 = \beta_r m_0 / \Omega_{r,j}$ ,  $z = \Gamma^{-1}$ ,

$$\Psi_i = \left( \beta_0 \frac{\Omega_{i,j}}{m_{i,j}} + 1 \right)^{-1} \quad \text{for } i = \{1, \dots, M\}, \quad (9)$$

$$H_t(\Psi) = \sum_{\ell_i \geq 0} \prod_{i=1, i \neq r}^M G_{\ell_i}(\Psi_i), \quad (10)$$

$$G_\ell(\Psi_i) = \begin{cases} 1 - p_i (1 - \Psi_i^{m_{i,j}}) & \text{for } \ell = 0 \\ \frac{p_i \Gamma(\ell + m_{i,j})}{\ell! \Gamma(m_{i,j})} \left( \frac{\Omega_{i,j}}{m_{i,j}} \right)^\ell \Psi_i^{m_{i,j} + \ell} & \text{for } \ell > 0. \end{cases} \quad (11)$$

In (11), the index  $i$  on the right hand side matches that of the argument  $\Psi_i$ , and  $j = \mathbf{g}(r)$  to coincide with the index of the serving sector antenna.

#### V. NETWORK POLICIES

##### A. Power Control

A typical power-allocation policy for DS-CDMA networks is to select the transmit power  $\{P_i\}$  for all mobiles in  $\mathcal{X}_j$  such that, after compensation for shadowing and power-law attenuation, each mobile's transmission is received at sector antenna  $S_j$  with the same power  $P_0$ . For such a power-control policy, each mobile in  $\mathcal{X}_j$  will transmit with a power  $P_i$  that satisfies

$$P_i 10^{\xi_{i,j}/10} f(\|S_j - X_i\|) = P_0, \quad X_i \in \mathcal{X}_j. \quad (12)$$

where  $f(\cdot)$  is given by (2). Since the reference mobile  $X_r \in \mathcal{X}_j$ , its transmit power is determined by (12). To accomplish the power-control policy, sector-antenna receivers estimate the average received powers of their associated mobiles. Feedback of these estimates enables the associated mobiles to change their transmitted powers so that all received powers are approximately equal [14].

For a reference mobile  $X_r$ , the interference at sector antenna  $S_j$  is from the mobiles in the set  $\mathcal{A}_j \setminus X_r$ . This set can be partitioned into two subsets. The first subset  $\mathcal{X}_j \setminus X_r$  comprises the *intracell interferers*, which are the other mobiles in the same cell and sector as the reference mobile. The second subset  $\mathcal{A}_j \setminus \mathcal{X}_j$  comprises the *intercell interferers*, which are the mobiles covered by sector antenna  $S_j$  but associated with a cell sector other than  $\mathcal{X}_j$ .

Considering intracell interference, all of the mobiles within the sector transmit with power given by (12). Since  $P_r$  and  $P_i$  are obtained from (12), the middle line of (6) gives the normalized mean received power of the intracell interferers:

$$\Omega_{i,j} = \frac{h}{G} 10^{\xi_{r,j}/10} \|S_j - X_r\|^{-\alpha}, \quad X_i \in \mathcal{X}_j \setminus X_r. \quad (13)$$

Although the number of mobiles  $M_j$  in the cell sector must be known to compute the outage probability, the locations of these mobiles in the cell are irrelevant to the computation of the  $\Omega_{i,j}$  of the intracell interferers.

Considering intercell interference, the set  $\mathcal{A}_j \setminus \mathcal{X}_j$  can be further partitioned into sets  $\mathcal{A}_j \cap \mathcal{X}_k, k \neq j$ , containing the mobiles covered by sector antenna  $S_j$  but associated with some other sector antenna  $S_k$ . For those mobiles in  $\mathcal{A}_j \cap \mathcal{X}_k$ , power control implies that

$$P_i 10^{\xi_{i,k}/10} f(\|S_k - X_i\|) = P_0, \quad X_i \in \mathcal{X}_k \cap \mathcal{A}_j, \quad k \neq j. \quad (14)$$

Substituting (14), (12) with  $i = r$ , and (2) into (6) yields

$$\Omega_{i,j} = \frac{h}{G} 10^{\xi_{i,j}/10} \left( \frac{\|S_j - X_i\| \|S_j - X_r\|}{\|S_k - X_i\|} \right)^{-\alpha} \\ \xi_{i,j} = \xi_{i,j} + \xi_{r,j} - \xi_{i,k}, \quad X_i \in \mathcal{X}_k \cap \mathcal{A}_j, \quad k \neq j \quad (15)$$

for  $\mathcal{A}_j \setminus \mathcal{X}_j$ , which gives the normalized mean intercell interference power at the reference sector antenna due to interference from mobile  $i$  of sector  $k = \mathbf{g}(i)$ .

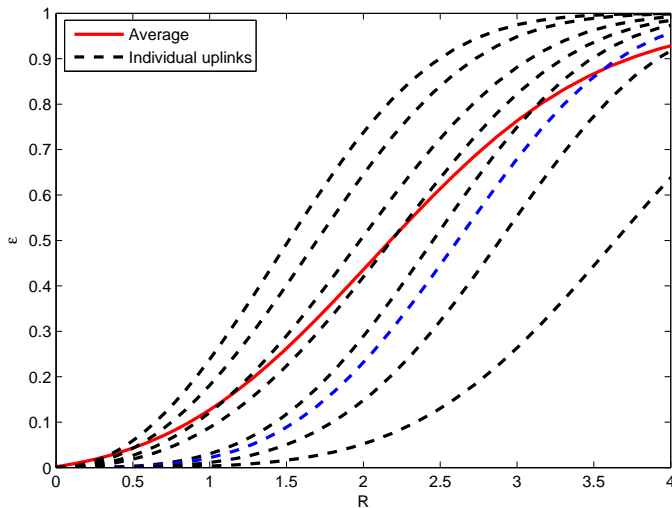


Fig. 2. Outage probability of eight randomly selected uplinks (dashed lines) along with the average outage probability for the entire network (solid line). The results are for a half-loaded network ( $M/C = G/2$ ) with distance-dependent fading and shadowing ( $\sigma_s = 8$  dB) and are shown as a function of the rate  $R$ .

### B. Rate Control

In addition to controlling the transmitted power, the rate  $R_i$  of each uplink needs to be selected. Due to the irregular network geometry, which results in cell sectors of variable areas and numbers of mobiles, the amount of received interference can vary dramatically from one sector antenna to another. With a fixed rate, or equivalently, a fixed SINR threshold  $\beta$  for each sector, the result is a highly variable outage probability. An alternative to using a fixed rate for the entire network is to adapt the rate of each uplink to satisfy an outage constraint or maximize the throughput of each uplink [15], [16].

To illustrate the influence of rate on performance, consider the following example. The network has  $C = 50$  base stations and  $M = 400$  mobiles placed in a circular network of radius  $r_{\text{net}} = 2$ . The base-station exclusion zones have radius  $r_{\text{bs}} = 0.25$ , and the mobile exclusion zones have radius  $r_{\text{m}} = 0.01$ . The spreading factor is  $G = 16$ , and the chip factor is  $h = 2/3$ . Since  $M/C = G/2$ , the network is characterized as being *half loaded*. The SNR is  $\Gamma = 10$  dB, the activity factor is  $p_i = 1$ , the path-loss exponent is  $\alpha = 3$ , and lognormal shadowing is assumed with standard deviation  $\sigma_s = 8$  dB. A *distance-dependent fading* model is assumed, where the Nakagami parameter  $m_{i,j}$  is

$$m_{i,j} = \begin{cases} 3 & \text{if } \|S_j - X_i\| \leq r_{\text{bs}}/2 \\ 2 & \text{if } r_{\text{bs}}/2 < \|S_j - X_i\| \leq r_{\text{bs}} \\ 1 & \text{if } \|S_j - X_i\| > r_{\text{bs}} \end{cases} \quad (16)$$

The distance-dependent-fading model characterizes the situations where mobiles close to the base station are in the line-of-sight, but mobiles farther away are not.

Fig. 2 shows the outage probability as a function of rate. Assuming the use of a capacity-approaching code, two-dimensional signaling over an AWGN channel, and Gaussian interference, the SINR threshold corresponding to rate  $R$  is  $\beta = 2^R - 1$ . The dashed lines in Fig. 2 were generated by selecting eight random uplinks and computing the outage prob-

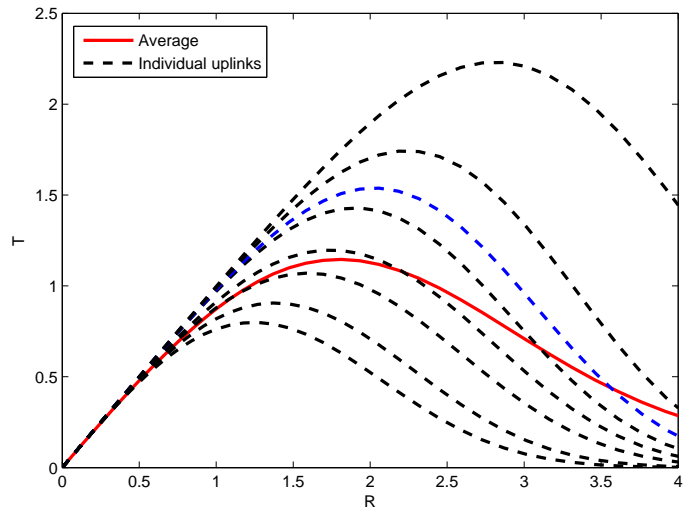


Fig. 3. Throughput of eight randomly selected uplinks (dashed lines) along with the average throughput for the entire network (solid line). System parameters are the same used to generate Fig. 2.

ability for each using this threshold. Despite the power control, there is considerable variability in the outage probability. The outage probabilities  $\{\epsilon_i\}$  were computed for all  $M$  uplinks in the system, and the average outage probability,

$$\mathbb{E}[\epsilon] = \frac{1}{M} \sum_{i=1}^M \epsilon_i \quad (17)$$

is displayed as a solid line in the figure.

Fig. 3 shows the *throughput* as a function of rate, where the throughput of the  $i^{\text{th}}$  uplink is found as

$$T_i = R_i(1 - \epsilon_i) \quad (18)$$

and represents the rate of successful transmissions. The parameters are the same as those used to produce Fig. 2, and again the SINR threshold corresponding to rate  $R$  is  $\beta = 2^R - 1$ . The plot shows the throughput for the same eight uplinks whose outages were shown in Fig. 2, as well as the average throughput

$$\mathbb{E}[T] = \frac{1}{M} \sum_{i=1}^M R_i(1 - \epsilon_i). \quad (19)$$

1) *Fixed-Rate Policies*: A fixed-rate policy requires that all uplinks in the system must use the same rate; i.e.,  $R_i = R$  for all uplinks. On the one hand, the rate could be selected to maximize the average throughput. With respect to the example shown in Fig. 3, this corresponds to selecting the  $R$  that maximizes the solid curve, which occurs at  $R = 1.81$ . However, at the rate that maximizes throughput, the corresponding outage probability could be unacceptably high. When  $R = 1.81$  in the example, the corresponding average outage probability is  $\mathbb{E}[\epsilon] = 0.37$ , which is too high for many applications. As an alternative to maximizing throughput, the rate  $R$  could be selected to satisfy an outage constraint  $\zeta$  so that  $\mathbb{E}[\epsilon] \leq \zeta$ . For instance, setting  $R = 0.84$  in the example satisfies an average outage constraint  $\zeta = 0.1$  with equality. To distinguish between the two fixed-rate policies, we call the first policy

*maximal-throughput fixed rate* (MTFR) and the second policy *outage-constrained fixed rate* (OCFR).

2) *Variable-Rate Policies*: If  $R$  is selected to satisfy an average outage constraint, the outage probability of the individual uplinks will vary around this average. Furthermore, selecting  $R$  to maximize the average throughput does not generally maximize the throughput of the individual uplinks. These issues can be alleviated by selecting the rates  $R_i$  independently for the different uplinks. The rates could be selected to require all uplinks to satisfy the outage constraint  $\zeta$ ; i.e.,  $\epsilon_i \leq \zeta$  for all  $i$ . We call this the *outage-constrained variable-rate* (OCVR) policy. Alternatively, the selection could be made to maximize the throughput of each uplink; i.e.,  $R_i = \arg \max T_i$  for each uplink, where the maximization is over all possible rates. We call this the *maximal-throughput variable-rate* (MTVR) policy. Both policies can be implemented by having the base station track the outage probabilities or throughputs of each uplink and feeding back rate-control commands to ensure that the target performance is achieved. The outage probability can be easily found by encoding the data with a cyclic-redundancy-check code and declaring an outage when a check fails.

For both variable-rate policies, we assume that the code rate is adapted by maintaining the duration of channel symbols while varying the number of information bits per symbol. The spreading factor  $G$  and symbol rate are held constant, so there is no change in bandwidth. However, a major drawback with rate control is that the rates required to maintain a specified outage probability varies significantly among the mobiles in the network. This variation results in low throughput for some mobiles, particularly those located at the edges of the cells, while other mobiles have a high throughput. Unequal throughputs may not be acceptable when a mobile may be stuck or parked near a cell edge for a long time, and an interior mobile may have more allocated throughput than it needs.

### C. Cell Association

The downlinks of a cellular DS-CDMA network use orthogonal spreading sequences. Because the number of orthogonal spreading sequences available to the cell sector is limited to  $G$  when sectorization is used for the downlinks, the number of served mobiles using  $S_j$  is limited to  $M_j \leq G$ . This limit then restricts the number of mobiles that have uplink service. If there are  $M_j > G$  mobiles, then some of these mobiles will either be refused service by  $S_j$  or given service at a lower rate (through the use of an additional time multiplexing). In the following, we consider two policies for handling this situation. With the first policy, which we call *denial policy*, the  $M_j - G$  mobiles whose path losses to the base station are greatest are denied service, in which case they do not appear in the set  $\mathcal{X}_j$  for any  $j$ , and their rates are set to zero. With the second policy, which we call *reselection policy*, each of the  $M_j - G$  mobiles in an overloaded cell sector attempts to connect to the sector antenna with the next-lowest path loss out to a maximum reassociation distance  $d_{\max}$ . If no suitably oriented sector antenna is available within distance  $d_{\max}$ , the mobile is denied service. The *denial* policy is the same as the *reselection* policy with  $d_{\max} = 0$ .

## VI. PERFORMANCE ANALYSIS

### A. Performance Metrics

While the outage probability, throughput, and rate characterize the performance of a single uplink, they do not quantify the total data flow in the network because they do not account for the number of uplink users that are served. By taking into account the number of mobiles per unit area, the total data flow in a given area can be characterized by the *area spectral efficiency*, defined as

$$\mathcal{A} = \lambda \mathbb{E}[T] = \lambda \mathbb{E}[(1 - \epsilon) R] \quad (20)$$

where  $\lambda = M/(\pi r_{\text{net}}^2)$  is the density of transmissions in the network, and the units are bits per channel use per unit area. Area spectral efficiency [9] can be interpreted as the spatial intensity of transmissions; i.e., the rate of successful data transmission per unit area.

Performance metrics are calculated by using a Monte Carlo approach with 1000 simulation trials as follows. In each simulation trial, a realization of the network is obtained by placing  $C$  base stations and  $M$  mobiles within the disk of radius  $r_{\text{net}}$  according to the uniform-clustering model with minimum base-station separation  $r_{\text{bs}}$  and minimum mobile separation  $r_{\text{m}}$ . The path loss from each base station to each mobile is computed by applying randomly generated shadowing factors. The set of mobiles associated with each cell sector is determined. Assuming that the number of mobiles served in a cell sector cannot exceed  $G$ , which is the number of orthogonal sequences available for the downlink, the rate of the last  $M_j - G$  mobiles in the cell sector (if there are that many) is determined by the cell association policy. At each sector antenna, the power-control policy is applied to determine the power the antenna receives from each mobile that it serves. In each cell sector, the rate-control policy is applied to determine the rate and threshold.

For each uplink, the outage probability is computed by applying the rate-control policy and using (8) – (11), (13), and (15). Equation (17) is applied to calculate the average outage probability for the network realization. Equation (18) is applied to calculate the throughputs according to the resource-allocation policy, and then (19) is applied to compute the average throughput for the network realization. Finally, multiplying by the density  $\lambda$  and averaging over all simulated network realizations yields the average outage probability  $\bar{\epsilon}$  and the average area spectral efficiency  $\bar{\mathcal{A}}$ .

Notice that the simulator only needs to randomly place the mobiles and base stations according to the spatial model and select the shadowing factors; i.e., it only needs to draw the *network realization*. The simulator does *not* need to draw the power gains  $\{g_{i,j}\}$ . Without applying the results of Section IV, the simulator would be far more complex because it would need to simulate the fading for every network realization. The number of power gains that would need to be generated could be as many as a million for every network realization, depending on the desired level of confidence. On the other hand, our approach not only avoids the unnecessary generation of power gains, it provides an *exact* result for any given network realization. In essence, the approach makes it possible

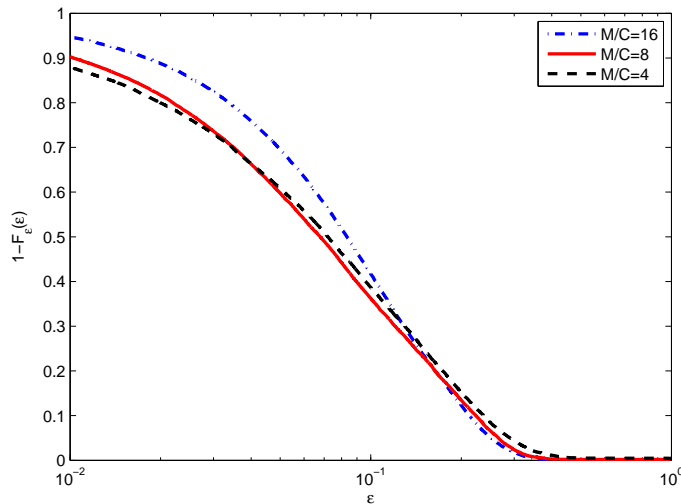


Fig. 4. Ccdf of the outage probability using an OCFR policy,  $R = 2$ , three network loads, distance-dependent fading, and shadowing.

to achieve the same results as a very detailed simulator, but can do so without needing to simulate the fading.

### B. Simulation Parameters

In the following subsections, the Monte Carlo method described in the previous subsection is used to characterize the uplink performance. In all cases considered, the network has  $C = 50$  base stations placed in a circular network of radius  $r_{\text{net}} = 2$ . Except for Subsection VI-G, which studies the influence of  $r_{\text{bs}}$ , the base-station exclusion zones are set to have radius  $r_{\text{bs}} = 0.25$ . A variable number  $M$  of mobiles are placed within the network using exclusion zones of radius  $r_m = 0.01$ . The SNR is  $\Gamma = 10$  dB, and the activity factor is  $p_i = 1$ . Unless otherwise stated, the path-loss exponent is  $\alpha = 3$ . Two fading models are considered: *Rayleigh fading*, where  $m_{i,j} = 1$  for all  $i$ , and *distance-dependent fading*, which is described by (16). Both unshadowed and shadowed ( $\sigma_s = 8$  dB) environments are considered. The chip factor is  $h = 2/3$ , and except for Subsection VI-F, which studies the influence of  $G$ , the spreading factor is  $G = 16$ . Except for Section VI-H,  $d_{\text{max}} = 0$ ; i.e., mobiles that overload sectors are denied service.

### C. Outage-Constrained Fixed-Rate Policy

As illustrated in Fig. 2, using an OCFR policy results in a high variability of outage probabilities. Fig. 4 illustrates the variability of  $\epsilon$  with respect to all uplinks and simulation trials under a OCFR policy by plotting its complementary cumulative distribution function (ccdf) with  $R = 2$ , three network loads, distance-dependent fading, and shadowing.

### D. Outage-Constrained Variable-Rate Policy

With the OCVR policy, the rate  $R_i$  (equivalently,  $\beta_i$ ) of each uplink is selected such that the outage probability does not exceed  $\zeta = 0.1$ . While the outage probability is fixed, the rates of the uplinks will be variable. Let  $\bar{R}$  denote the average rate over all uplinks and simulation trials. In Fig.

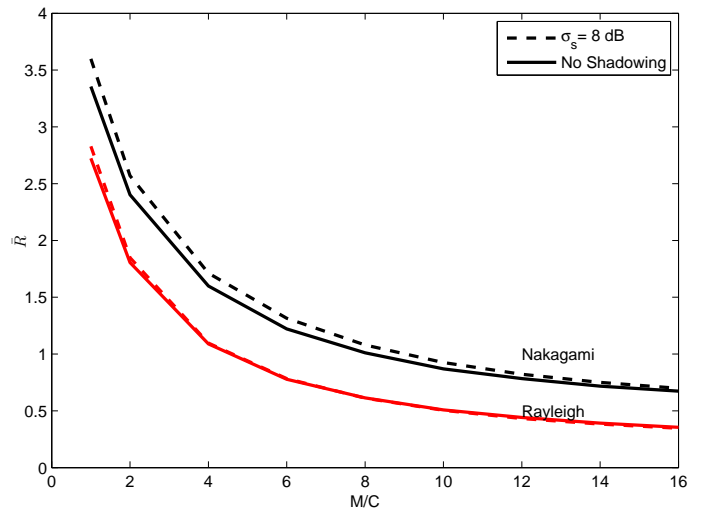


Fig. 5. Average rate of the OCVR policy as function of the load  $M/C$  for both Rayleigh and distance-dependent Nakagami fading, and both shadowed ( $\sigma_s = 8$  dB) and unshadowed cases.

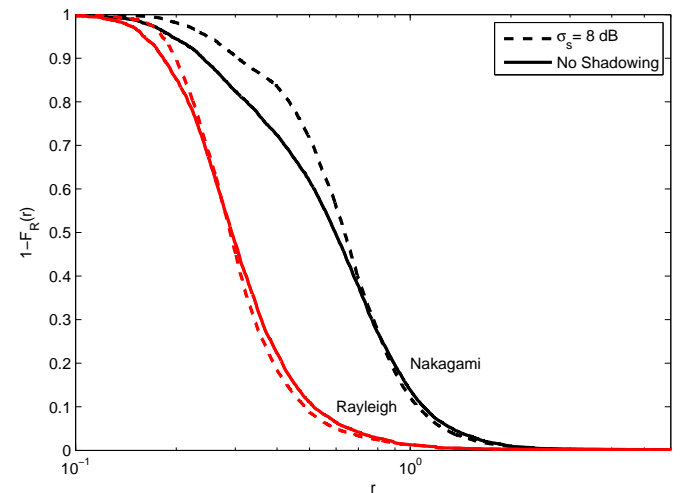


Fig. 6. Ccdf of the rate for fully-loaded system ( $M/C = G$ ) under the OCVR policy in Rayleigh and distance-dependent Nakagami fading, and both shadowed ( $\sigma_s = 8$  dB) and unshadowed cases.

5,  $\bar{R}$  is shown as a function of the load  $M/C$ . In Fig. 6, the variability of  $R_i$  is illustrated by showing the ccdf of the rate for a fully-loaded system ( $M/C = G = 16$ ) in both Rayleigh fading and distance-dependent fading, and both with and without shadowing. The fairness of the system can be determined from this figure, which shows the percentage of uplinks that meet a particular rate requirement.

### E. Policy Comparison

Fig. 7 shows the average area spectral efficiency  $\bar{\mathcal{A}}$  of the four network policies in distance-dependent fading, both with and without shadowing, as a function of the load  $M/C$ . For the OCFR policy, the optimal rate was determined for each simulation trial and then  $\bar{\mathcal{A}}$  was computed by averaging over 1000 trials. For the OCVR policy, the uplink rate  $R_i$  of each uplink was maximized subject to an outage constraint. While the area spectral efficiencies of the MTFR and MTVR policies are potentially superior to those of the OCFR and OCVR

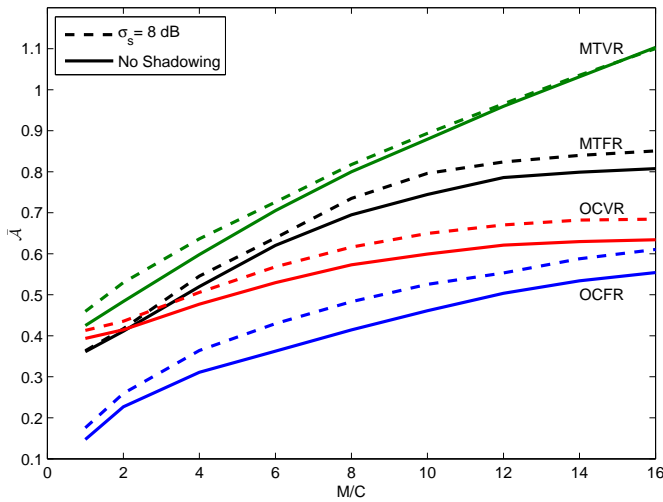


Fig. 7. Average area spectral efficiency for the four network policies as function of the load  $M/C$  for distance-dependent fading and both shadowed ( $\sigma_s = 8$  dB) and unshadowed cases.

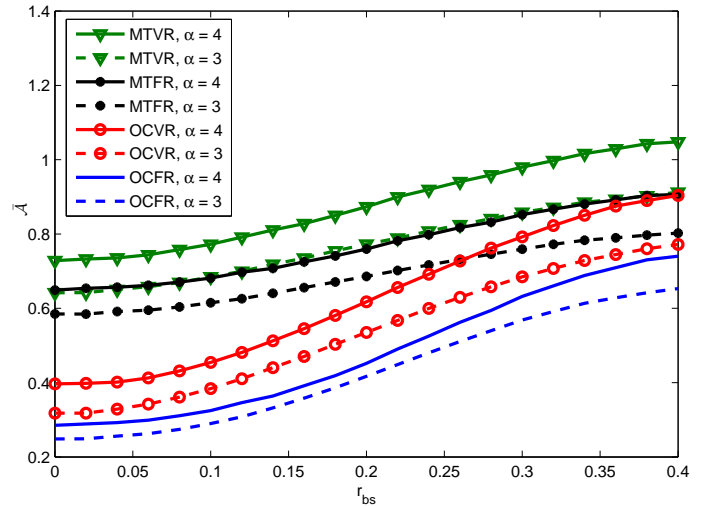


Fig. 9. Average area spectral efficiency as a function of the base-station exclusion-zone radius  $r_{bs}$  for four policies and two values of path-loss exponent  $\alpha$ .

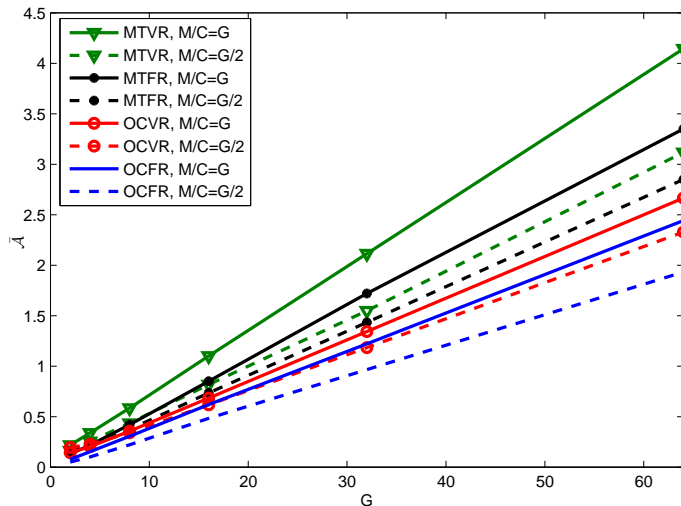


Fig. 8. Average area spectral efficiency as function of spreading factor  $G$  for two values of system load, distance-dependent fading, and shadowing with  $\sigma_s = 8$  dB.

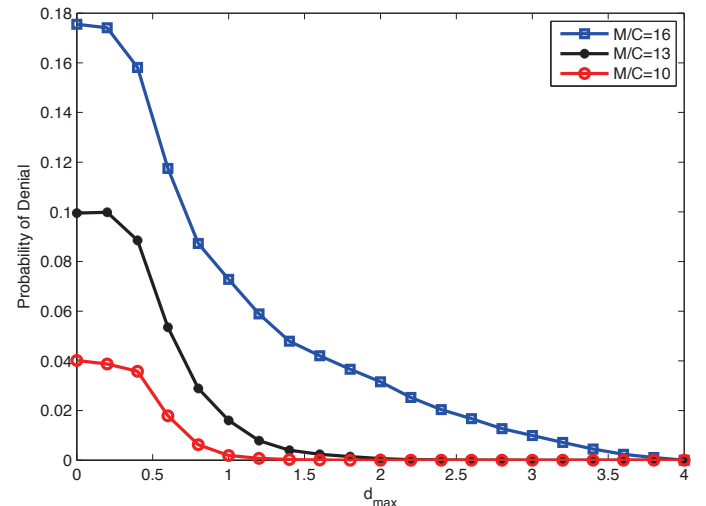


Fig. 10. Probability that a mobile is denied service due to cell overload as a function of the maximum reselection distance  $d_{max}$ .

policies, this advantage comes at the cost of a variable and high value of  $\epsilon$ , which is generally too large for most applications. The OCVR policy has a higher average area spectral efficiency than the OCFR policy.

#### F. Spreading factor

Fig. 8 shows  $\bar{A}$  as a function of the spreading factor  $G$  (with  $h = 2/3$ ) for the shadowed distance-dependent-fading channel. Two loads are shown for each of the four policies. An increase in  $G$  is beneficial for all policies, but the MTRV policy benefits the most.

#### G. Base-station Exclusion Zone

Fig. 9 shows  $\bar{A}$  for each of the four policies as a function of the base-station exclusion-zone radius  $r_{bs}$  for  $M/C = G/2$  and two values of path-loss exponent  $\alpha$ . The distance-dependent fading model is used, and shadowing is applied

with  $\sigma_s = 8$  dB. The two policies that constrain the outage probability are more sensitive to the value of  $r_{bs}$  than the two policies that maximize throughput. An increase in  $\alpha$  increases  $\bar{A}$  for all four policies.

#### H. Cell Association

In the previously shown results, mobiles were denied service if they were in an overloaded sector. By allowing mobiles to reselect base stations out to a distance of  $d_{max}$ , the probability that they are denied service due to overload can be reduced. Fig. 10 shows the probability that a mobile is denied service due to sector overload as a function of the maximum reselection distance  $d_{max}$  for three different values of average cell load  $M/C$ . By setting  $d_{max}$  sufficiently large, the probability that a mobile is denied service due to overload can be made arbitrarily small. The tradeoff for keeping these mobiles connected is that  $\bar{A}$  decreases because mobiles must



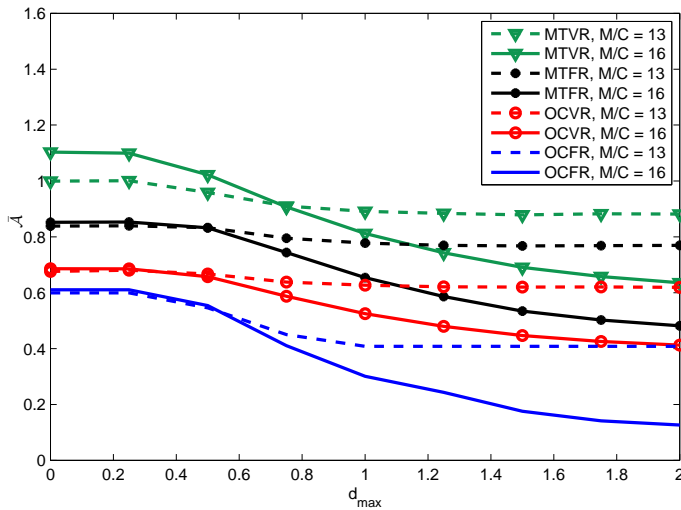


Fig. 11. Average area spectral efficiency as a function of the maximum reselection distance  $d_{\max}$ .

transmit at a higher power, thereby causing more interference. This tradeoff is illustrated in Fig. 11, which shows  $\bar{A}$  as a function of  $d_{\max}$  for all four policies and two system loads. In general,  $\bar{A}$  decreases with increasing  $d_{\max}$ , and the decrease is more pronounced for the more heavily loaded system.

## VII. CONCLUSION

A new analysis of DS-CDMA uplinks has been presented. This analysis is much more detailed and accurate than existing ones and facilitates the resolution of network design issues. In particular, it has been shown that once power control is established, the rate can be allocated according to a fixed-rate or variable-rate policy with the objective of either maximizing throughput or meeting an outage constraint. An advantage of variable-rate power control is that it allows an outage constraint to be enforced on every uplink, which is impossible when a fixed rate is used throughout the network. Another advantage is an increased area spectral efficiency.

## REFERENCES

- [1] K. S. Gilhousen et al., "On the capacity of a cellular CDMA system," *IEEE Trans. Veh. Technol.*, vol. 40, pp. 303–312, May 1991.
- [2] A. J. Viterbi, *CDMA Principles of Spread Spectrum Communication*. Addison-Wesley, 1995.
- [3] M. Zorzi, "On the Analytical Computation of the Interference Statistics with Applications to the Performance Evaluation of Mobile Radio Systems," *IEEE Trans. Commun.*, vol. 45, pp. 103–109, Jan. 1997.
- [4] J. Andrews, F. Baccelli, and R. K. Ganti, "A tractable approach to coverage and rate in cellular networks," *IEEE Trans. Commun.*, vol. 59, pp. 3122–3134, Nov. 2011.
- [5] B. Błaszczyszyn, M.K. Karray, M. K. and H. P. Keeler, "Using Poisson processes to model lattice cellular networks," *Proc. INFOCOM*, Apr. 2013.
- [6] H. S. Dhillon, T. D. Novlan, and J. G. Andrews, "Coverage probability of uplink cellular networks," *Proc. GLOBECOM*, Dec. 2012.
- [7] S. Stoyan, W. Kendall, and J. Mecke, *Stochastic Geometry and Its Applications*. Wiley, 1996.
- [8] F. Baccelli and B. Błaszczyszyn, *Stochastic Geometry and Wireless Networks*. NOW: Foundations and Trends in Networking, 2010.
- [9] S. Weber, J. G. Andrews, and N. Jindal, "An overview of the transmission capacity of wireless networks," *IEEE Trans. Commun.*, vol. 58, pp. 3593–3604, Dec. 2010.

- [10] D. Torrieri and M. C. Valenti, "The outage probability of a finite ad hoc network in Nakagami fading," *IEEE Trans. Commun.*, vol. 60, pp. 3509–3518, Nov. 2012.
- [11] M. C. Valenti, D. Torrieri, and S. Talarico, "A New Analysis of the DS-CDMA Cellular Downlink Under Spatial Constraints," *Proc. IEEE Int. Conf. on Comp., Network. and Commun.*, (San Diego, Ca), Jan. 2013.
- [12] D. Torrieri, *Principles of Spread-Spectrum Communication Systems, 2nd ed.* Springer, 2011.
- [13] D. Torrieri, "Performance of direct-sequence systems with long pseudonoise sequences," *IEEE J. Selected Areas Commun.*, vol. 10, pp. 770–781, May 1992.
- [14] L. Zhao and J. W. Mark, "Multi-step closed-loop power control using linear receivers for DS-CDMA systems," *IEEE Trans. Wireless Commun.*, 2004, vol. 3, pp. 2141–2155, Nov. 2004.
- [15] C. C. Chai, T. T. Tjhung, and L. C. Leck, "Combined power and rate adaptation for wireless cellular systems," *IEEE Trans. Wireless Commun.*, vol.4, pp. 6–13, Jan. 2005.
- [16] A. Subramanian and A. H. Sayed, "Joint rate and power control algorithms for wireless networks," *IEEE Trans. Signal Process.*, 2005, vol. 53, pp. 4204–4214, Nov. 2005.



award for sustained contributions to the field.

**Don Torrieri** is a research engineer and Fellow of the US Army Research Laboratory. His primary research interests are communication systems, adaptive arrays, and signal processing. He received the Ph. D. degree from the University of Maryland. He is the author of many articles and several books including *Principles of Spread-Spectrum Communication Systems*, 2nd ed. (Springer, 2011). He has taught many graduate courses at Johns Hopkins University and many short courses. In 2004, he received the Military Communications Conference achievement



served as a track or symposium co-chair for VTC-Fall-2007, ICC-2009, Milcom-2010, ICC-2011, and Milcom-2012, and has served as an editor for *IEEE Transactions on Wireless Communications* and *IEEE Transactions on Vehicular Technology*. His research interests are in the areas of communication theory, error correction coding, applied information theory, wireless networks, simulation, and secure high-performance computing. His research is funded by the NSF and DoD. He is registered as a Professional Engineer in the State of West Virginia.

**Matthew C. Valenti** is a Professor in Lane Department of Computer Science and Electrical Engineering at West Virginia University. He holds BS and Ph.D. degrees in Electrical Engineering from Virginia Tech and a MS in Electrical Engineering from the Johns Hopkins University. From 1992 to 1995 he was an electronics engineer at the US Naval Research Laboratory. He serves as an associate editor for *IEEE Wireless Communications Letters* and as Vice Chair of the Technical Program Committee for Globecom-2013. Previously, he has



and optimization of ad-hoc and cellular networks.

**Salvatore Talarico** received the BSc and MEng degrees in electrical engineering from University of Pisa, Italy, in 2006 and 2007 respectively. From 2008 until 2010, he worked in the R&D department of Screen Service Broadcasting Technologies (SSBT) as an RF System Engineer. He is currently a research assistant and a Ph.D. student in the Lane Department of Computer Science and Electrical Engineering at West Virginia University, Morgantown, WV. His research interests are in wireless communications, software defined radio and modeling, performance